



Mathematical Modeling of Schistosomiasis Transmission Using Reaction-Diffusion Equations

Dhorasso Temfack^{1,†}, ¹School of Computer Science and Statistics, Trinity College Dublin, Ireland

†temfackd@tcd.ie

Article Information

Keywords: Disease dynamics; Human behavior; Neglected tropical disease; Reaction-diffusion equations; Schistosomiasis; Sensitivity analysis

AMS 2020 Classification: 34D20; 34D23; 35R99; 92B05; 92D30

Abstract

Schistosomiasis, a neglected tropical disease caused by parasitic trematodes of the genus *Schistosoma*, affects millions of people in tropical and subtropical regions lacking access to clean water and proper hygiene. With its impact on health and well-being, the World Health Organization aspires to eliminate schistosomiasis by 2030. This work addresses the challenge of effective control in endemic areas by integrating diffusion in each sub-population using reaction-diffusion equations. The proposed model includes treated individuals who have undergone massive drug administration and a time-dependent function that models the change in human behavior. We present a Partial Differential Equation (PDE) model of schistosomiasis spread that incorporates population movement and human behavior change. Mathematical analysis explores the system's dynamics according to the infection threshold R_0 , shedding light on the disease's behavior. Sensitivity analysis is used to identify the key parameters affecting disease spread. Numerical simulations under different scenarios elucidate the impact of human behavior on disease dynamics. This research contributes to a deeper understanding of schistosomiasis transmission and provides insights into control strategies.

1. Introduction

Schistosomiasis, also known as Bilharzia or snail fever, is a neglected tropical disease (NTD) prevalent in tropical and subtropical countries with limited access to safe drinking water and proper hygiene. It is caused by trematode blood flukes of the genus *Schistosoma* and is endemic in 52 countries, affecting over 290 million people in 2018 [1]. The World Health Organization (WHO) has aimed to eliminate schistosomiasis as a public health problem by 2030 [2]. Schistosomiasis is transmitted through contact with fresh water contaminated by the infective larvae of *Schistosoma* parasites [1]. The life cycle of the disease involves the release of parasite eggs into water bodies through human waste, hatching of eggs into miracidia, infecting snails, developing into cercariae and eventually infecting humans through skin penetration, leading to organ damage, abdominal pain, blood in stool or urine, anemia, dysuria and other health complications [3, 4]. Effective control of schistosomiasis remains challenging in endemic regions and the main approach is mass drug administration (MDA) using praziquantel, an anthelmintic drug, to reduce morbidity, mortality and transmission rates [5].

Research into the dynamics of *Schistosoma* infections traces its origins back to 1965 when George Macdonald introduced the inaugural mathematical framework for schistosome epidemiology [6]. This pioneering model, based on differential equations, describes the progression of the average worm burden in the human host, taking into account the complex nature of schistosome. Subsequent to this, researchers have developed the model taking into account the heterogeneity of the intermediate host [7]. Contemporary investigations have leveraged agent-based models (ABMs) and individual-based models (IBMs) to capture the multifaceted diversity in human behaviors and interactions [8, 9]. These innovative models have not only illuminated the pivotal role of water-related activities but have also pinpointed regions of heightened transmission risk [8]. However, human behavior and the movement of individuals between locations, play a significant role in disease spread, as infected individuals can introduce the parasite to new areas, potentially creating new transmission hotspots [10]. Since then, various models have been proposed that include more detailed information such as spatial heterogeneity or seasonality [10, 11]. Zhang et al. [12] studied the spatial distribution of schistosomiasis and the treatment needs in Africa. Manuela Ciddio et al. [10] utilized a multidimensional network model to investigate the spatial spread of schistosomiasis within the Saint-Louis region of

Senegal. The study emphasizes the crucial role of spatial connectivity in disease propagation and underscores the significance of accounting for various transport pathways to develop effective disease control strategies.

This paper aims to develop a mathematical model for schistosomiasis spread based on reaction-diffusion equations that integrate human behavior change. Reaction-diffusion systems have proven to be effective and appropriate modeling tools for comprehending the spatiotemporal dynamics of diseases. Operating within the domain of spatial continuity, these systems have been pivotal in delving into intricate topics such as nonlinear infection mechanisms and spatial diffusivity. The model we present in this paper takes into account individuals who have undergone mass drug administration (MDA) as detailed in [13]. Moreover, our investigation extends to encompass changes in human behavior and the exploration of diffusion phenomena, contributing to an enhanced understanding of the spatial distribution of the disease.

The remainder of this work is organized as follows. Section 2 presents a Partial Differential Equation (PDE) model that incorporates population mobility and the biological description of the infection parameters. A mathematical analysis of the model to understand the dynamical behavior of the system depending on the value of the threshold of infection R_0 is done in Section 3. Section 4 conducts the sensitivity analysis of R_0 to identify parameters sensitive to the disease spread. Section 5 presents the numerical simulations under different scenarios by taking appropriate parameters to explore the effect of human behavior on disease dynamics. Finally, Section 6 gives a brief discussion and conclusion.

2. Model Formulation

Models of schistosomiasis transmission typically incorporate various aspects of the schistosome life cycle. The populations considered consist of humans (H) and snails (S), with the presence of cercariae (C) and miracidia (M). Cercariae (C) represent larval worms shed into the aquatic environment by infected snails, while miracidia (M) are eggs shed into streams by infected humans engaging in activities like fishing, swimming, or drinking. The human population is divided into sub-populations: susceptible (S_h), exposed (E_h), infected (I_h) and treated (T_h) individuals, while the snail population consists of susceptible (S_s), exposed (E_s) and infected (I_s) snails. The susceptible human reproduces at a constant rate Λ_h and dies naturally at the rate μ_h . The susceptible become infected through contact with fresh water contaminated by cercariae from infected snail at the rate $\beta_{ch}\theta C$. The exposed humans become infectious at a rate γ_h and we assume that a rate σ_h of infected humans receives the MDA, while a fraction λ recovers and returns to the susceptible class. Others may die because of the infections at a rate ρ_h . We assume that the treated humans are not infectious, i.e., they do not produce eggs for miracidia. Shedding of infection within the environment by infected humans is assumed to occur at rate α_m which represents the rate of miracidia produced by infected humans. Susceptible snails reproduce at a constant rate Λ_s and die naturally at the rate μ_s . They become infected upon contact with miracidia from the shedding of infected humans and mammals at the rate $\beta_{ms}M$. The exposed snails become infectious at a rate γ_s and those infected snails shed larva worms (cercariae) in the environment at a rate α_c . The death rates of miracidia and cercariae are μ_m and μ_c , respectively. The model assumes no immigration of infectious individuals. Figure 1 illustrates the transmission diagram of Schistosomiasis.

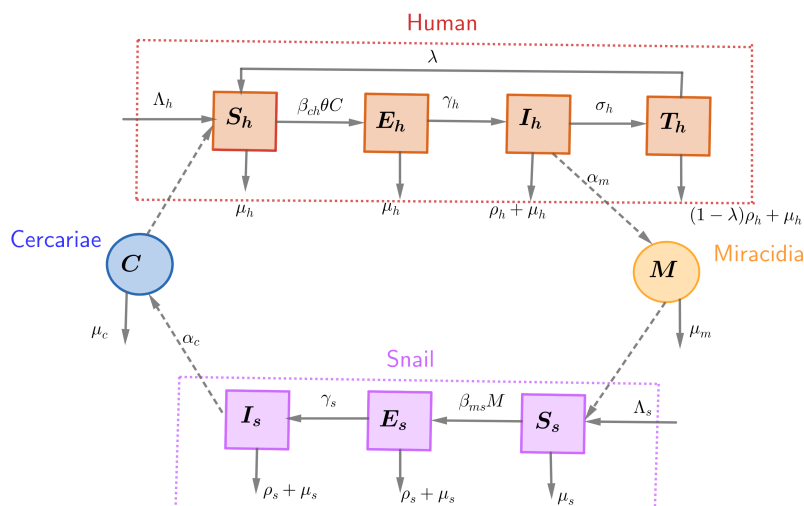


Figure 1: Transmission dynamics of Schistosomiasis. The disease cycle begins when infected individuals release *Schistosoma* eggs into freshwater bodies through feces or urine. These eggs hatch, releasing miracidia that infect snails, where they develop into cercariae. The cercariae are then released into the water, actively seeking contact with human skin. Upon skin penetration, they enter the bloodstream and migrate to the liver, maturing into adult worms. The worms then migrate to the veins of the urinary or intestinal systems, where they lay eggs, which starts the whole cycle again. Direct transitions between compartments are represented by the horizontal solid arrows. The mortality rate is represented by the vertical arrows exiting the compartments. The dashed arrow from C to S_h and from M to S_s indicates the contact of susceptible humans with freshwater contaminated by cercariae and the contact of susceptible snails with miracidia, respectively. On the other hand, the dashed arrow from I_h to M and from I_s to C indicates the shedding rate of miracidia and cercariae, respectively.

We assume that snails, miracidia and cercariae can move within their environment due to factors such as water currents, host movements and other ecological interactions. Diffusion processes allow us to simulate the movement of these populations over time, which affects how they encounter and interact with each other.

This leads to the following system of partial differential equations:

$$\left\{ \begin{array}{l} \frac{\partial S_h(x,t)}{\partial t} = d_1 \Delta S_h + \Lambda_h + \lambda T_h - \beta_{ch} \theta(t) C S_h - \mu_h S_h, \\ \frac{\partial E_h(x,t)}{\partial t} = d_2 \Delta E_h + \beta_{ch} \theta(t) C S_h - \gamma_h E_h - \mu_h E_h, \\ \frac{\partial I_h(x,t)}{\partial t} = d_3 \Delta I_h + \gamma_h E_h - \sigma_h I_h - \rho_h I_h - \mu_h I_h, \\ \frac{\partial T_h(x,t)}{\partial t} = d_4 \Delta T_h + \sigma_h I_h - \lambda T_h - (1 - \lambda) \rho_h T_h - \mu_h T_h, \\ \frac{\partial M(x,t)}{\partial t} = d_5 \Delta M + \alpha_m I_h - \mu_m M, \\ \frac{\partial S_s(x,t)}{\partial t} = d_6 \Delta S_s + \Lambda_s - \beta_{ms} M S_s - \mu_s S_s, \\ \frac{\partial E_s(x,t)}{\partial t} = d_7 \Delta E_s + \beta_{ms} M S_s - \gamma_s E_s - \rho_s E_s - \mu_s E_s, \\ \frac{\partial I_s(x,t)}{\partial t} = d_8 \Delta I_s + \gamma_s E_s - \rho_s I_s - \mu_s I_s, \\ \frac{\partial C(x,t)}{\partial t} = d_9 \Delta C + \alpha_c I_s - \mu_c C. \end{array} \right. \quad (2.1)$$

Where S_h , E_h , I_h and T_h , represent the populations of susceptible, exposed, infected and treated humans at position x and time t , respectively. S_s , E_s , and I_s represent the populations of susceptible, exposed and infected snails at position x and time t , respectively. M and C represent the populations of miracidia and cercariae at position x and time t . We assume that the human, snail, miracidia and cercariae population moves in the region Ω according to Fick's second law [14], with d_i ($i = 1, \dots, 9$), being the diffusion coefficients. Each diffusion coefficient d_i determines how quickly each sub-population spreads through space. The Laplacian operator Δ represents the spatial diffusion between neighboring locations and computes the difference between a compartment's value at a specific location and the average of its neighboring compartments.

By incorporating the model the time-dependent function $\theta(t)$ into the model, we identified human behavioral changes such as avoiding wading, swimming and other forms of contact with contaminated water, as well as adopting improved sanitation and gaining access to clean water. This function is given by

$$\theta(t) = \begin{cases} 1 & \text{No intervention,} \\ (1 + \zeta e^{rt})^{-1} & \text{with intervention} \end{cases} \quad (2.2)$$

This type of function is often used to capture the gradual change in behavior from initial resistance to eventual widespread adoption [15]. Here, ζ represents the maximum level of behavior change effectiveness that can be achieved. We have $\zeta \in (0, 1)$, where 0 represents no behavior change, 1 represents full behavior change compliance and r determines how quickly behavior change is adopted and becomes effective over time.

The following initial conditions are associated with the system (2.1) :

$$\left\{ \begin{array}{l} S_h(x, 0) = \phi_1(x), E_h(x, 0) = \phi_2(x), I_h(x, 0) = \phi_3(x), T_h(x, 0) = \phi_4(x), M(x, 0) = \phi_5(x), \\ S_s(x, 0) = \phi_6(x), E_s(x, 0) = \phi_7(x), I_s(x, 0) = \phi_8(x), C(x, 0) = \phi_9(x), \\ x \in \Omega \text{ and } \phi_i \in C^2(\Omega) \cap C(\Omega), i = 1, \dots, 9, \end{array} \right. \quad (2.3)$$

and homogeneous Neumann boundary conditions are imposed:

$$\frac{\partial S_h}{\partial \eta} = \frac{\partial E_h}{\partial \eta} = \frac{\partial I_h}{\partial \eta} = \frac{\partial T_h}{\partial \eta} = \frac{\partial M}{\partial \eta} = \frac{\partial S_s}{\partial \eta} = \frac{\partial E_s}{\partial \eta} = \frac{\partial I_s}{\partial \eta} = \frac{\partial C}{\partial \eta} = 0, \quad x \in \partial\Omega, t > 0, \quad (2.4)$$

where Ω is an open bounded subset of \mathbb{R}^n with a smooth boundary $\partial\Omega$ and η is the unit outer normal to $\partial\Omega$. The biological description of all the parameters in the system (2.1) is given in Table 1.

Table 1: Description of the model parameters.

Param.	Biological description	Value	Unit	Source
Λ_h	Recruitment rate of humans	0.62	humans per day	[16]
Λ_s	Recruitment rate of snails	2.5	snails per day	[16]
β_{ch}	Infection rate of cercariae on humans	4×10^{-6}	per day	[10]
β_{ms}	Infection rate of miracidia on snails	5×10^{-5}	per day	[10]
θ	Time-dependent function describing human intervention	-	-	-
ρ_h	Death rate of humans due to infection	0.000274	per day	[13]
ρ_s	Death rate of snails due to infection	0.011	per day	[10]
γ_h	Rate of transmission of humans from exposure to infection	0.0238	per day	[13]
γ_s	Rate of transmission of snails from exposure to infection	0.0286	per day	[13]
σ_h	Transmission rate of humans from infection to treatment	0.03	per day	[17]
α_m	Rate individuals produce miracidia	6.96	miracidia per human per day	[18]
α_c	Rate snails produce cercariae	2.6	cercariae per snail per day	[18]
λ	Treatment efficacy (for <i>Schistosoma mansoni</i>)	0.767	-	[19]
μ_h	Natural death rate of humans	0.00004379	per day	[13]
μ_s	Natural death rate of snails	2.7×10^{-3}	per day	[10]
μ_m	Natural death rate of miracidia	3.04	per day	[10]
μ_c	Natural death rate of cercariae	0.91	per day	[10]

3. Mathematical Analysis of the Model

This section is devoted to the theoretical study of the transmission model of the spread of Schistosomiasis described by a system of 9-PDE of the system (2.1). The existence and uniqueness of positive solutions and the existence of equilibria and their stability are established depending on the value of the basic reproduction number.

The system (2.1) can be expressed as:

$$\frac{\partial X(x,t)}{\partial t} = DX(x,t) + f(X(x,t)), \tag{3.1}$$

with $X = (S_h, E_h, I_h, T_h, M, S_s, E_s, I_s, C)$, $D = \text{diag}(d_1, d_2, d_3, d_4, d_5, d_6, d_7, d_8, d_9)$, and function f represent the right hand side of the system (2.1) without the diffusive part, i.e.

$$f(X(x,t)) = \begin{pmatrix} \Lambda_h + \lambda T_h - \beta_{ch}\theta CS_h - \mu_h S_h, \\ \beta_{ch}\theta CS_h - \gamma_h E_h - \mu_h E_h, \\ \gamma_h E_h - \sigma_h I_h - \rho_h I_h - \mu_h I_h, \\ \sigma_h I_h - \lambda T_h - (1 - \lambda)\rho_h T_h - \mu_h T_h, \\ \alpha_m I_h - \mu_m M, \\ \Lambda_s - \beta_{ms} MS_s - \mu_s S_s, \\ \beta_{ms} MS_s - \gamma_s E_s - \rho_s E_s - \mu_s E_s, \\ \gamma_s E_s - \rho_s I_s - \mu_s I_s, \\ \alpha_c I_s - \mu_c C \end{pmatrix}. \tag{3.2}$$

3.1. Existence, Uniqueness and Positivity

We said that $X^- = (S_h^-, E_h^-, I_h^-, T_h^-, M^-, S_s^-, E_s^-, I_s^-, C^-)$ and $X^+ = (S_h^+, E_h^+, I_h^+, T_h^+, M^+, S_s^+, E_s^+, I_s^+, C^+)$ and in $C(\bar{\Omega} \times [0, \infty)) \cap C^{1,2}(\Omega \times [0, \infty))$ are lower and upper solutions of system (2.1), respectively, if $X^- \leq X^+$ in $\bar{\Omega} \times [0, \infty)$ and the following differential inequalities hold:

$$\begin{cases} \frac{\partial X^-(x,t)}{\partial t} \leq DX^-(x,t) + f(X^-(x,t)), \\ \frac{\partial X^+(x,t)}{\partial t} \geq DX^+(x,t) + f(X^+(x,t)), \end{cases} \text{ for } (x,t) \in \Omega \times (0, \infty) \tag{3.3}$$

and

$$\begin{cases} \frac{\partial X^-}{\partial \eta} \leq 0 \leq \frac{\partial X^+}{\partial \eta}, & \text{for } (x, t) \in \partial\Omega \times (0, \infty), \\ X^-(x, t) \leq \Phi(x, t) \leq X^+(x, t) & \text{for } (x, t) \in \bar{\Omega} \times (0, \infty). \end{cases} \quad (3.4)$$

Where \leq is the standard order relation in \mathbb{R}^n ($x \leq y \Leftrightarrow x_i \leq y_i$, for $i = 1, \dots, n$) and $\Phi = (\phi_1, \phi_2, \phi_3, \phi_4, \phi_5, \phi_6, \phi_7, \phi_8, \phi_9)$.

Theorem 3.1. *Let suppose that the initial functions ϕ_i ($i = 1, 2, \dots, 9$) are continuous in Ω . Then problem (2.1) has exactly one regular solution $X(x, t) = (S_h(x, t), E_h(x, t), I_h(x, t), T_h(x, t), M(x, t), S_s(x, t), E_s(x, t), I_s(x, t), C(x, t))$. This solution is characterized by positivity and boundedness in the region $\Omega \times [0, \infty)$.*

Proof. The existence and uniqueness of the solution are obtained using the Lemma 1 in [20].

Let $\Gamma := C(\Omega, \mathbb{R})$. We observe that $0_{\mathbb{R}^9} = (0, 0, 0, 0, 0, 0, 0, 0, 0)$ and $W = (w_1, w_2, w_3, w_4, w_5, w_6, w_7, w_8, w_9)$ are respectively lower and upper solutions of the system (2.1), where

$$\begin{aligned} w_1 &= \max \left\{ \frac{\Lambda_h}{\mu_h}, \|\phi_1\|_{\Gamma} \right\}, & w_6 &= \max \left\{ \frac{\Lambda_s}{\mu_s}, \|\phi_6\|_{\Gamma} \right\}, \\ w_2 &= \max \left\{ \frac{\Lambda_h}{\mu_h}, \|\phi_2\|_{\Gamma} \right\}, & w_7 &= \max \left\{ \frac{\Lambda_s}{\mu_s}, \|\phi_7\|_{\Gamma} \right\}, \\ w_3 &= \max \left\{ \frac{\gamma_h \Lambda_h}{\mu_h^2}, \|\phi_3\|_{\Gamma} \right\}, & w_8 &= \max \left\{ \frac{\gamma_s \Lambda_s}{\mu_s^2}, \|\phi_8\|_{\Gamma} \right\}, \\ w_4 &= \max \left\{ \frac{\sigma_h \gamma_h \Lambda_h}{\mu_h^3}, \|\phi_4\|_{\Gamma} \right\}, & w_9 &= \max \left\{ \frac{\alpha_c \Lambda_s}{\mu_c \mu_s}, \|\phi_9\|_{\Gamma} \right\}, \\ w_5 &= \max \left\{ \frac{\alpha_m \Lambda_h}{\mu_m \mu_h}, \|\phi_5\|_{\Gamma} \right\}. \end{aligned} \quad (3.5)$$

By applying the Redinger's Lemma, we conclude that the problem (2.1) has exactly one regular solution $X(x, t)$ such that $0_{\mathbb{R}^9} \leq X(x, t) \leq W$ in $\Omega \times [0, \infty)$.

Hence, $0 \leq S_h(x, t) \leq w_1$, $0 \leq E_h(x, t) \leq w_2$, $0 \leq I_h(x, t) \leq w_3$, $0 \leq T_h(x, t) \leq w_4$, $0 \leq M(x, t) \leq w_5$, $0 \leq S_s(x, t) \leq w_6$, $0 \leq E_s(x, t) \leq w_7$, $0 \leq I_s(x, t) \leq w_8$, $0 \leq C(x, t) \leq w_9$.

Furthermore, if $\phi_i(x) \neq 0$ for $i = 1, \dots, 9$, then from the maximum principle, we have $S_h(x, t) > 0$, $E_h(x, t) > 0$, $I_h(x, t) > 0$, $T_h(x, t) > 0$, $M(x, t) > 0$, $S_s(x, t) > 0$, $E_s(x, t) > 0$, $I_s(x, t) > 0$, $C(x, t) > 0$ for all $t > 0$, $x \in \Omega$. \square

3.2. Equilibria and Basic Reproduction Number

3.2.1. Equilibria

The equilibria of the system (2.1) are found by solving

$$\frac{dX(t)}{dt} = f(X(t)) = 0, \quad (3.6)$$

with $X = (S_h, E_h, I_h, T_h, M, S_s, E_s, I_s, C)$ and f given by (3.2). Hence, the system (2.1) has two equilibrium points, namely the disease-free equilibrium point (DFE) and endemic equilibrium point (EE).

1. The DFE is given by

$$E^0 = (S_h^0, 0, 0, 0, 0, S_s^0, 0, 0, 0) = \left(\frac{\Lambda_h}{\mu_h}, 0, 0, 0, 0, \frac{\Lambda_s}{\mu_s}, 0, 0, 0 \right),$$

and it translates to the ideal case where the disease disappears into the human and snail population and always exists.

2. The EE is given by $E^* = (S_h^*, E_h^*, I_h^*, T_h^*, M^*, S_s^*, E_s^*, I_s^*, C^*)$, where

$$\begin{cases} S_h^* = \frac{\mu_c(\rho_s + \mu_s)(\gamma_s + \rho_s + \mu_s)(\beta_{ms}\alpha_m I_h^* + \mu_s\mu_m)(\lambda + (1-\lambda)\rho_h + \mu_h)\Lambda_h + \lambda\sigma_h I_h^*}{\gamma_s\beta_{ms}\alpha_m\alpha_c\Lambda_s(\lambda + (1-\lambda)\rho_h + \mu_h)I_h^* + \mu_h\mu_c(\rho_s + \mu_s)(\gamma_s + \rho_s + \mu_s)(\beta_{ms}\alpha_m I_h^* + \mu_s\mu_m)}, \\ E_h^* = \frac{\sigma_h + \rho_h + \mu_h}{\gamma_h} I_h^*, \\ I_h^* = \frac{\gamma_h}{\mu_h\mu_s\mu_c\mu_m(\gamma_h + \mu_h)(\rho_s + \mu_s)(\sigma_h + \rho_h + \mu_h)(\gamma_s + \rho_s + \mu_s)(\lambda + (1-\lambda)\rho_h + \mu_h)(R_e - 1)}, \\ T_h^* = \frac{\sigma_h}{\lambda + (1-\lambda)\rho_h + \mu_h} I_h^*, \\ M^* = \frac{\alpha_m}{\mu_m} I_h^*, \\ S_s^* = \frac{\mu_m\Lambda_s}{\beta_{ms}\alpha_m I_h^* + \mu_s\mu_m}, \\ E_s^* = \frac{\beta_{ms}\alpha_m\Lambda_s}{(\gamma_s + \rho_s + \mu_s)(\beta_{ms}\alpha_m I_h^* + \mu_s\mu_m)} I_h^*, \\ I_s^* = \frac{\gamma_s\beta_{ms}\alpha_m\Lambda_s}{(\rho_s + \mu_s)(\gamma_s + \rho_s + \mu_s)(\beta_{ms}\alpha_m I_h^* + \mu_s\mu_m)} I_h^*, \\ C^* = \frac{\gamma_s\beta_{ms}\alpha_m\alpha_c\Lambda_s}{\mu_c(\rho_s + \mu_s)(\gamma_s + \rho_s + \mu_s)(\beta_{ms}\alpha_m I_h^* + \mu_s\mu_m)} I_h^*. \end{cases} \tag{3.7}$$

With

$$\begin{aligned} R_e &= \frac{\beta_{ch}\theta\beta_{ms}\alpha_c\alpha_m\gamma_h\gamma_s\Lambda_h\Lambda_s}{\mu_h\mu_s\mu_c\mu_m(\gamma_h + \mu_h)(\rho_s + \mu_s)(\sigma_h + \rho_h + \mu_h)(\gamma_s + \rho_s + \mu_s)}, \\ A_1 &= \gamma_s\beta_{ch}\theta\beta_{ms}\alpha_m\alpha_c\Lambda_s(\rho_h\sigma_h((1-\lambda)\rho_h + \mu_h) + (\lambda + (1-\lambda)\rho_h + \mu_h)(\gamma_h(\rho_s + \mu_s) + \mu_h(\sigma_h + \rho_h + \mu_h))), \\ A_2 &= \alpha_m\mu_h\mu_c\beta_{ms}(\gamma_h + \mu_h)(\rho_s + \mu_s)(\sigma_h + \rho_h + \mu_h)(\gamma_s + \rho_s + \mu_s)(\lambda + (1-\lambda)\rho_h + \mu_h). \end{aligned}$$

This equilibrium translates the situation of persistence of the disease into the population and exists if $R_e > 1$.

3.2.2. Basic reproduction number

The epidemiological concept of the basic reproduction number (R_0) pertains to the average count of fresh infections within a susceptible population caused by a single infectious individual (human or snail). To determine this metric we use the same approach as [21] and compute the next generation matrix.

Let the infective compartment be $X_I = (E_h, I_h, M, E_s, I_s, C)$, considering the following system:

$$\begin{cases} \frac{\partial E_h(x,t)}{\partial t} = d_2\Delta E_h + \beta_{ch}\theta CS_h - \gamma_h E_h - \mu_h E_h, \\ \frac{\partial I_h(x,t)}{\partial t} = d_3\Delta I_h + \gamma_h E_h - \sigma_h I_h - \rho_h I_h - \mu_h I_h, \\ \frac{\partial M(x,t)}{\partial t} = d_5\Delta M + \alpha_m I_h - \mu_m M, \\ \frac{\partial E_s(x,t)}{\partial t} = d_7\Delta E_s + \beta_{ms}MS_s - \gamma_s E_s - \rho_s E_s - \mu_s E_s, \\ \frac{\partial I_s(x,t)}{\partial t} = d_8\Delta I_s + \gamma_s E_s - \rho_s I_s - \mu_s I_s, \\ \frac{\partial C(x,t)}{\partial t} = d_9\Delta C + \alpha_c I_s - \mu_c C. \end{cases} \tag{3.8}$$

Let's consider the two vectors F and V . Where F represents the rate of new infections appearing in a compartment and V represents the rate of infectives leaving the system, defined as follows:

$$F = \begin{pmatrix} \beta_{ch}\theta CS_h \\ 0 \\ 0 \\ \beta_{ms}S_s \\ 0 \\ 0 \end{pmatrix}, \quad \text{and } V = \begin{pmatrix} (\gamma_h + \mu_h)E_h \\ (\sigma_h + \rho_h + \mu_h)I_h - \gamma_h E_h \\ \mu_m M - \alpha_m I_h \\ (\gamma_s + \rho_s + \mu_s)E_s \\ (\rho_s + \mu_s)I_s - \gamma_s E_s \\ \mu_c C - \alpha_c I_s \end{pmatrix}.$$

The Jacobian matrices of F and V at the DFE E^0 are given by:

$$J_F = \begin{pmatrix} 0 & 0 & 0 & 0 & 0 & \frac{\beta_{ch}\theta\Lambda_h}{\mu_h} \\ 0 & 0 & 0 & 0 & 0 & 0 \\ 0 & 0 & 0 & 0 & 0 & 0 \\ 0 & 0 & \frac{\beta_{ms}\Lambda_s}{\mu_s} & 0 & 0 & 0 \\ 0 & 0 & 0 & 0 & 0 & 0 \\ 0 & 0 & 0 & 0 & 0 & 0 \end{pmatrix}, \quad J_V = \begin{pmatrix} \gamma_h + \mu_h & 0 & 0 & 0 & 0 & 0 \\ -\gamma_h & \sigma_h + \rho_h + \mu_h & 0 & 0 & 0 & 0 \\ 0 & -\alpha_m & \mu_m & 0 & 0 & 0 \\ 0 & 0 & 0 & \gamma_s + \rho_s + \mu_s & 0 & 0 \\ 0 & 0 & 0 & -\gamma_s & \rho_s + \mu_s & 0 \\ 0 & 0 & 0 & 0 & -\alpha_c & \mu_c \end{pmatrix}.$$

Then, the next generation matrix is given by:

$$J_F J_V^{-1} = \begin{pmatrix} 0 & 0 & 0 & \frac{\beta_{ch}\theta\Lambda_h\alpha_c\gamma_c}{\mu_h\mu_c(\gamma_s+\rho_s+\mu_s)(\rho_s+\mu_s)} & \frac{\beta_{ch}\theta\mu_h\alpha_c}{\mu_h\mu_c(\rho_s+\mu_s)} & \frac{\beta_{ch}\theta\Lambda_h}{\mu_h\mu_c} \\ 0 & 0 & 0 & 0 & 0 & 0 \\ 0 & 0 & 0 & 0 & 0 & 0 \\ \frac{\beta_{ms}\Lambda_s\alpha_m}{\mu_s(\gamma_h+\mu_h)(\sigma_h+\rho_h+\mu_h)} & \frac{\beta_{ms}\Lambda_s\alpha_m}{\mu_s\mu_m(\sigma_h+\rho_h+\mu_h)} & \frac{\beta_{ms}\Lambda_s}{\mu_s\mu_m} & 0 & 0 & 0 \\ 0 & 0 & 0 & 0 & 0 & 0 \\ 0 & 0 & 0 & 0 & 0 & 0 \end{pmatrix}.$$

The reproduction number is the spectral radius of the next generation matrix. Hence, we have

$$R_0 := \rho(J_F J_V^{-1}) = \left(\frac{\beta_{ch}\theta\beta_{ms}\alpha_c\alpha_m\gamma_h\gamma_s\Lambda_h\Lambda_s}{\mu_h\mu_s\mu_c\mu_m(\gamma_h+\mu_h)(\rho_s+\mu_s)(\sigma_h+\rho_h+\mu_h)(\gamma_s+\rho_s+\mu_s)} \right)^{\frac{1}{2}}. \tag{3.9}$$

Using the notations

$$R_{0,hs} = \frac{\beta_{ms}\alpha_m\gamma_s\Lambda_s}{\mu_s\mu_m(\rho_s+\mu_s)(\gamma_s+\rho_s+\mu_s)}, \text{ and } R_{0,sh} = \frac{\beta_{ch}\theta\alpha_c\gamma_h\Lambda_h}{\mu_h\mu_c(\gamma_h+\mu_h)(\sigma_h+\rho_h+\mu_h)}, \tag{3.10}$$

the expression of R_0 takes the form:

$$R_0 = \sqrt{R_{0,hs} \cdot R_{0,sh}}. \tag{3.11}$$

The quantity $R_{0,hs}$ and $R_{0,sh}$ reflect the transmission from human to snail and from snail to human, respectively. This expression of R_0 as a geometric mean of $R_{0,hs}$ and $R_{0,sh}$, effectively demonstrates how the different population parameters in the life cycle (Human-Snail-Human), such as birth, death and infection rates impact the transmission intensity as shown in Section 4.

Lemma 3.2. *If $R_0 > 1$, then the endemic equilibrium point E^* of system (2.1) given by (3.7) exists and is unique.*

Proof. It is easy to observe that $R_e = R_0^2$. Hence $R_e > 1$ if and only if $R_0 > 1$. Therefore the necessary and sufficient condition for the existence of the endemic equilibrium E^* is $R_0 > 1$. □

The nature of the system (2.1) is determined by the time-dependent intervention function $\theta(t)$. The analysis of the stability of the system is divided into two cases: one where there is no human intervention ($\theta(t) = 1$) and the other where there is human intervention ($\theta(t) = (1 + \zeta e^{rt})^{-1}$).

3.3. Stability of autonomous dynamical system

3.3.1. Local stability of the equilibrium

To establish the local stability of the equilibrium, A similar methodology as in prior works such as [22, 23] is employed. Consider the eigenvalues of $-\Delta$ on Ω with homogeneous Neumann boundary conditions: $0 = v_0 < v_i < v_{i+1}$, $i = 1, 2, \dots$ and $E(v_i)$ the associated eigenspace. Let denote by \mathbb{B}_i , the orthogonal basis for $E(v_i)$. Consequently, the solution space $\mathbb{B} = \{(S_h, E_h, I_h, T_h, M, S_s, E_s, I_s, C)\}$ of the system (2.1) can be partitioned as follows:

$$\mathbb{B} = \bigoplus_{i=1}^{\infty} \mathbb{B}_i.$$

If we denote by $J(E)$ the Jacobian matrix of the system (2.1) at the equilibrium E , then as prove in [24] the eigenvalues of $J(E)$ are equivalent to the eigenvalue of the matrix

$$M(E) = -v_i D + J_f(E).$$

Where $D = \text{diag}(d_1, d_2, d_3, d_4, d_5, d_6, d_7, d_8, d_9)$ is a diagonal matrix of the diffusion coefficients and $J_f(E)$ is the Jacobian matrix of the function f given in (3.2) at the equilibrium E .

Theorem 3.3. *If $R_0 < 1$ and $\theta(t) = 1$, then the disease-free equilibrium point E^0 of system (2.1) is locally asymptotically stable (LAS).*

Proof. Let $J(E^0)$ the Jacobian matrix of the system (2.1) at the DFE. The eigenvalue value of $J(E^0)$ are equivalent to that the matrix

$$M(E^0) = -v_i D + J_f(E^0) = \begin{pmatrix} -a_1 & 0 & 0 & \lambda & 0 & 0 & 0 & 0 & -\beta_{ch}\theta\frac{\Lambda_h}{\mu_h} \\ 0 & -a_2 & 0 & 0 & 0 & 0 & 0 & 0 & \beta_{ch}\theta\frac{\Lambda_h}{\mu_h} \\ 0 & \gamma_h & -a_3 & 0 & 0 & 0 & 0 & 0 & 0 \\ 0 & 0 & \sigma_h & -a_4 & 0 & 0 & 0 & 0 & 0 \\ 0 & 0 & \alpha_m & 0 & -a_5 & 0 & 0 & 0 & 0 \\ 0 & 0 & 0 & 0 & -\beta_{ms}\frac{\Lambda_s}{\mu_s} & -a_6 & 0 & 0 & 0 \\ 0 & 0 & 0 & 0 & \beta_{ms}\frac{\Lambda_s}{\mu_s} & 0 & -a_7 & 0 & 0 \\ 0 & 0 & 0 & 0 & 0 & 0 & \gamma_s & -a_8 & 0 \\ 0 & 0 & 0 & 0 & 0 & 0 & 0 & \alpha_c & -a_9 \end{pmatrix}.$$

Where $a_1 = \mu_h + v_i d_1$, $a_2 = (\gamma_h + \mu_h) + v_i d_2$, $a_3 = (\sigma_h + \rho_h + \mu_h) + v_i d_3$, $a_4 = (\lambda + (1 - \lambda)\rho_h + \mu_h) + v_i d_4$, $a_5 = \mu_m + v_i d_5$, $a_6 = \mu_s + v_i d_6$, $a_7 = (\sigma_s + \rho_s + \mu_s) + v_i d_7$, $a_8 = (\rho_s + \mu_s) + v_i d_8$ and $a_9 = \mu_c + v_i d_9$.

The characteristic polynomial of this matrix is given by:

$$P_1(x) = -(a_1 + x)(a_4 + x)(a_6 + x)Q_1(x) \quad \text{with}$$

$Q_1(x) = x^6 + k_5x^5 + k_4x^4 + k_3x^3 + k_2x^2 + k_1x + k_0$ and the values of the coefficients are:

$$\begin{aligned} k_0 &= a_2 a_3 a_5 a_7 a_8 a_9 \left(1 - \frac{\beta_{ch}\theta\beta_{ms}\alpha_c\alpha_m\gamma_h\gamma_s\Lambda_h\Lambda_s}{\mu_h\mu_s a_2 a_3 a_5 a_7 a_8 a_9} \right), \\ k_1 &= a_2 a_3 a_5 a_7 a_8 + a_2 a_3 a_5 a_7 a_9 + a_2 a_3 a_5 a_8 a_9 + a_2 a_3 a_7 a_8 a_9 + a_2 a_5 a_7 a_8 a_9 + a_3 a_5 a_7 a_8 a_9 > 0, \\ k_2 &= a_2 a_3 a_5 a_7 + a_2 a_3 a_5 a_8 + a_2 a_3 a_5 a_9 + a_2 a_3 a_7 a_8 + a_2 a_3 a_7 a_9 + a_2 a_3 a_8 a_9 + a_2 a_5 a_7 a_8 \\ &+ a_2 a_5 a_7 a_9 + a_2 a_5 a_8 a_9 + a_3 a_5 a_7 a_8 + a_3 a_5 a_7 a_9 + a_3 a_5 a_8 a_9 + a_5 a_7 a_8 a_9 > 0, \\ k_3 &= a_2 a_3 a_7 + a_2 a_3 a_8 + a_2 a_3 a_9 + a_2 a_5 a_7 + a_2 a_5 a_8 + a_2 a_5 a_9 + a_3 a_5 a_7 + a_3 a_5 a_8 + a_3 a_5 a_9 + a_5 a_7 a_8 \\ &+ a_5 a_7 a_9 + a_5 a_8 a_9 + a_2 a_7 a_8 + a_2 a_7 a_9 + a_2 a_8 a_9 + a_3 a_7 a_8 + a_3 a_7 a_9 + a_3 a_8 a_9 + a_7 a_8 a_9 > 0, \\ k_4 &= a_2 a_7 + a_2 a_8 + a_2 a_9 + a_3 a_7 + a_3 a_8 + a_3 a_9 + a_7 a_8 + a_7 a_9 + a_8 a_9 > 0, \\ k_5 &= a_2 + a_3 + a_5 + a_7 + a_8 + a_9 > 0. \end{aligned}$$

It is easy to see that P_1 has three negative eigenvalues: $x_1 = -a_1$, $x_2 = -a_4$ and $x_3 = -a_6$. The other eigenvalues are roots of $Q_1(x)$.

Since $k_1, k_2, k_3, k_4, k_5 > 0$, then by using the Routh-Hurwitz criteria [25] and the conditions of Hefferman [26] that the polynomial $Q_1(x)$ has negative real roots if $k_5 k_4 > k_3$, $k_4 k_2 > k_0$, $k_2 k_1 > k_3 k_0$. We already have:

$$\begin{aligned} k_5 k_4 - k_3 &= a_2^2 a_7 + a_2^2 a_8 + a_2^2 a_9 + a_2 a_3 a_7 + a_2 a_3 a_8 + a_2 a_3 a_9 + a_2 a_5 a_7 + a_2 a_5 a_8 \\ &+ a_2 a_5 a_9 + a_3 a_7 a_8 + a_3 a_7 a_9 + a_3 a_8 a_9 + a_5 a_7 a_8 + a_5 a_7 a_9 + a_5 a_8 a_9 \\ &> 0. \end{aligned}$$

If $R_0 < 1$, then we have:

$$\frac{\beta_{ch}\theta\beta_{ms}\alpha_c\alpha_m\gamma_h\gamma_s\Lambda_h\Lambda_s}{\mu_h\mu_s a_2 a_3 a_5 a_7 a_8 a_9} \leq R_0^2 < 1 \Rightarrow 0 < k_0 < a_2 a_3 a_5 a_7 a_8 a_9. \tag{3.12}$$

Hence,

$$k_4 k_2 > a_2 a_3 a_5 a_7 a_8 a_9 > k_0, \quad \text{and} \quad k_2 k_1 - k_3 k_0 > k_2 k_1 - a_2 a_3 a_5 a_7 a_8 a_9 k_3 = 0. \tag{3.13}$$

Thus all the eigenvalues of P_1 have a negative real part, which implies that the disease-free equilibrium E^0 is locally asymptotically stable if $R_0 < 1$. □

Theorem 3.4. *If $R_0 > 1$ and $\theta(t) = 1$, then the endemic equilibrium point E^* of system (2.1) is locally asymptotically stable (LAS).*

Proof. Let $J(E^*)$ the Jacobian matrix of the system (2.1) at the EE. The eigenvalue value of $J(E^*)$ are equivalent to that the matrix

$$M(E^*) = v_i D + J_f(E^*) = \begin{pmatrix} -b_1 & 0 & 0 & \lambda & 0 & 0 & 0 & 0 & -\beta_{ch}\theta S_h^* \\ \beta_{ch}\theta C^* & -b_2 & 0 & 0 & 0 & 0 & 0 & 0 & \beta_{ch}\theta S_h^* \\ 0 & \gamma_h & -b_3 & 0 & 0 & 0 & 0 & 0 & 0 \\ 0 & 0 & \sigma_h & -b_4 & 0 & 0 & 0 & 0 & 0 \\ 0 & 0 & \alpha_m & 0 & -b_5 & 0 & 0 & 0 & 0 \\ 0 & 0 & 0 & 0 & -\beta_{ms}S_s^* & -b_6 & 0 & 0 & 0 \\ 0 & 0 & 0 & 0 & \beta_{ms}S_s^* & 0 & -b_7 & 0 & 0 \\ 0 & 0 & 0 & 0 & 0 & 0 & \gamma_s & -b_8 & 0 \\ 0 & 0 & 0 & 0 & 0 & 0 & 0 & \alpha_c & -b_9 \end{pmatrix}.$$

Where $b_1 = \beta_{ch}\theta C^* + \mu_h + v_i d_1$, $b_2 = (\gamma_h + \mu_h) + v_i d_2$, $b_3 = (\sigma_h + \rho_h + \mu_h) + v_i d_3$, $b_4 = (\lambda + (1 - \lambda)\rho_h + \mu_h) + v_i d_4$, $b_5 = \mu_m + v_i d_5$, $b_6 = \beta_{ms}M^* + \mu_s + v_i d_6$, $b_7 = -\beta_{ms}M^* + (\sigma_s + \rho_s + \mu_s) + v_i d_7$, $b_8 = (\rho_s + \mu_s) + v_i d_8$ and $b_9 = \mu_c + v_i d_9$.

We are employing the approach as [27, 28, 29]. Assuming the linearized equation at the equilibrium point E^* takes the form:

$$U' = M(E^*)U, \quad (3.14)$$

Here, we consider a solution characterized by the expression:

$$U(t) = U_0 e^{tz}, \quad z \in \mathbb{C}^9, \quad (3.15)$$

where $U_0 = (U_1, U_2, U_3, U_4, U_5, U_6, U_7, U_8, U_9)$. Upon substituting this particular solution form (3.15) into the linearized system (3.14), we obtain the relationship $zU = M(E^*)U$, which can be rephrased as the subsequent system:

$$\begin{cases} zU_1 = -b_1 U_1 + \lambda U_4 - \beta_{ch}\theta S_h^* U_9, \\ zU_2 = \beta_{ch}\theta C^* U_1 - b_2 U_2 + \beta_{ch}\theta S_h^* U_9, \\ zU_3 = \gamma_h U_2 - b_3 U_3, \\ zU_4 = \sigma_h U_3 - b_4 U_4, \\ zU_5 = \alpha_m U_3 - b_5 U_5, \\ zU_6 = -\beta_{ms}S_s^* U_5 - b_6 U_6, \\ zU_7 = \beta_{ms}S_s^* U_5 - b_7 U_7, \\ zU_8 = \gamma_s U_7 - b_8 U_8, \\ zU_9 = \alpha_c U_8 - b_9 U_9. \end{cases} \quad (3.16)$$

The system (3.16) can be rewritten as

$$(1 + F_i(z))U_i + G_i(U) = (HU)_i, \quad i = 1, \dots, 9 \quad (3.17)$$

where

$$F_1(z) = \frac{1}{b_1}, \quad F_2(z) = \frac{1}{b_2}, \quad F_3(z) = \frac{1}{b_3}, \quad F_4(z) = \frac{1}{b_4}, \quad F_5(z) = \frac{1}{b_5}, \\ F_7(z) = \frac{1}{b_6}, \quad F_7(z) = \frac{1}{b_7}, \quad F_8(z) = \frac{1}{b_8}, \quad F_9(z) = \frac{1}{b_9},$$

and

$$G_1(U) = \frac{\beta_{ch}\theta S_h^*}{b_1} U_9, \quad G_6(U) = \frac{\beta_{ms}S_s^*}{b_6} U_5, \\ G_2(U) = G_3(U) = G_4(U) = G_5(U) = G_7(U) = G_8(U) = G_9(U) = 0,$$

and a non-negative matrix H given by

$$H = \begin{pmatrix} 0 & 0 & 0 & \frac{\lambda}{b_1} & 0 & 0 & 0 & 0 & 0 \\ \frac{\beta_{ch}\theta C^*}{b_1} & 0 & 0 & 0 & 0 & 0 & 0 & 0 & \frac{\beta_{ch}\theta S_h^*}{b_2} \\ 0 & \frac{\gamma_h}{b_3} & 0 & 0 & 0 & 0 & 0 & 0 & 0 \\ 0 & 0 & \frac{\sigma_h}{b_4} & 0 & 0 & 0 & 0 & 0 & 0 \\ 0 & 0 & \frac{\alpha_m}{b_5} & 0 & 0 & 0 & 0 & 0 & 0 \\ 0 & 0 & 0 & 0 & 0 & 0 & 0 & 0 & 0 \\ 0 & 0 & 0 & 0 & \frac{\beta_{ms}S_s^*}{b_7} & 0 & 0 & 0 & 0 \\ 0 & 0 & 0 & 0 & 0 & 0 & \frac{\gamma_s}{b_8} & 0 & 0 \\ 0 & 0 & 0 & 0 & 0 & 0 & 0 & \frac{\alpha_c}{b_9} & 0 \end{pmatrix}.$$

The equilibrium state denoted as $E^* = (S_h^*, E_h^*, I_h^*, T_h^*, M^*, S_s^*, E_s^*, I_s^*, C^*)$ is defined as the endemic equilibrium, satisfying the condition $E^* = HE^*$. Since all the components of E^* are positive when $R_0 > 1$. Let U denote a solution of equation (3.17), there exists a minimal positive real c_0 (as established in [29]), such that the following inequality holds:

$$|U| \leq c_0 E^*, \tag{3.18}$$

where $|U| = (|U_1|, |U_2|, |U_3|, |U_4|, |U_5|, |U_6|, |U_7|, |U_8|, |U_9|)$. The objective is to demonstrate $Re(z) < 0$. Let us assume by contradiction that $Re(z) \geq 0$.

Given that $U \neq 0$, we conclude that $Re(z) > 0$, leading to $|1 + F_i(z)| > 1$ for all $i = 1, \dots, 9$. Hence

$$\frac{c_0}{\Psi(z)} < c_0, \text{ where } \Psi(z) = \min_{i=1, \dots, 8} |1 + F_i(z)| > 1.$$

Hence, by the minimality of c_0 , it is follows that:

$$|U| > \frac{c_0}{\Psi(z)} E^*. \tag{3.19}$$

By applying the norm to both sides of the third equation in (3.17) and using the non-negativity of matrix H , we get:

$$|1 + F_3(z)||U_3| = |(HU)_3| \leq H|U_3| \leq c_0 H(E^*)_3 = c_0 I_h^*, \tag{3.20}$$

This implies that $|U_3| \leq \frac{c_0}{\Psi(z)} I_h^*$ and then, contradicts equation (3.19). Hence, $Re(z) < 0$, which means that all eigenvalues of the matrix $M(E^*)$ have a negative real part. Therefore, the endemic equilibrium E^* is locally asymptotically stable if $R_0 > 1$. \square

3.3.2. Global stability of the disease-free equilibrium

Theorem 3.5. *If $\theta(t) = 1$, then disease-free equilibrium point E^0 of system (2.1) is globally asymptotically stable (GAS) if $R_0 < 1$ and unstable if $R_0 > 1$.*

Proof. The Lyapunov-LaSalle technique is used to prove the global asymptotic stability of E^0 . Let's consider the Lyapunov function defined as follows :

$$L = \int_{\Omega} [c_1 E_h(x, t) + c_2 I_h(x, t) + c_3 M(x, t) + c_4 E_s(x, t) + c_5 I_s(x, t) + c_6 C(x, t)] dx, \tag{3.21}$$

where

$$\begin{aligned} c_1 &= \alpha_m \alpha_c \gamma_h \gamma_s \beta_s \Lambda_s (\gamma_h + \mu_h), \\ c_2 &= \alpha_m \alpha_c \gamma_s \beta_s \Lambda_s (\gamma_h + \mu_h) \\ c_3 &= \alpha_c \gamma_s \beta_s \Lambda_s (\gamma_h + \mu_h) (\sigma_h + \rho_h + \mu_h), \\ c_4 &= \alpha_c \gamma_s \mu_m \mu_s (\gamma_h + \mu_h) (\sigma_h + \rho_h + \mu_h), \\ c_5 &= \mu_m \mu_s (\rho_s + \mu_s) (\gamma_h + \mu_h) (\gamma_s + \rho_s + \mu_s) (\sigma_h + \rho_h + \mu_h), \\ c_6 &= \mu_m \mu_s \alpha_c (\gamma_h + \mu_h) (\gamma_s + \rho_s + \mu_s) (\sigma_h + \rho_h + \mu_h). \end{aligned}$$

We have:

$$\begin{aligned} \frac{dL}{dt} &= \int_{\Omega} \left[c_1 \frac{\partial E_h(x, t)}{\partial t} + c_2 \frac{\partial I_h(x, t)}{\partial t} + c_3 \frac{\partial M(x, t)}{\partial t} + c_4 \frac{\partial E_s(x, t)}{\partial t} + c_5 \frac{\partial I_s(x, t)}{\partial t} + c_6 \frac{\partial C(x, t)}{\partial t} \right] dx \\ &= \int_{\Omega} [c_1 (d_2 \Delta E_h + \beta_{ch} \theta C S_h - (\gamma_h + \mu_h E_h) E_h) + c_2 (d_3 \Delta I_h + \gamma_h E_h - (\sigma_h + \rho_h + \mu_h) I_h) \\ &+ c_3 (d_5 \Delta M + \alpha_m I_h - \mu_m M) + c_4 (d_7 \Delta E_s + \beta_{ms} M S_s - (\gamma_s + \rho_s + \mu_s) E_s) \\ &+ c_5 (d_8 \Delta I_s + \gamma_s E_s - (\rho_s + \mu_s) I_s) + c_6 (d_9 \Delta C + \alpha_c I_s - \mu_c C)] dx \\ &= \int_{\Omega} \left[c_1 \beta_h \left(S_h - \frac{c_6 \mu_c}{c_1 \beta_h} \right) C + (c_2 \gamma_h - c_1 (\gamma + \mu_h)) E_h + (c_3 \alpha_m - c_2 (\sigma_h + \rho_h + \mu_h)) I_h \right. \\ &+ (c_5 \gamma_s - c_4 (\gamma_s + \rho_s + \mu_s)) E_s + (c_6 \alpha_c - c_5 (\rho_s + \mu_s)) I_s + c_4 \beta_s \left(S_s - \frac{c_3 \mu_m}{c_4 \beta_s} \right) M \left. \right] dx \\ &+ \int_{\Omega} [c_1 d_2 \Delta E_h + c_2 d_3 \Delta I_h + c_3 d_5 \Delta M + c_4 d_7 \Delta E_s + c_5 d_8 \Delta I_s + c_6 d_9 \Delta C] dx \end{aligned}$$

According to the Green's formula and the homogeneous Neumann boundary conditions (2.4), we have

$$\int_{\Omega} \Delta E_h dx = \int_{\Omega} \Delta I_h dx = \int_{\Omega} \Delta M dx = \int_{\Omega} \Delta E_s dx = \int_{\Omega} \Delta I_s dx = \int_{\Omega} \Delta C dx = 0,$$

Hence

$$\begin{aligned} \frac{dL}{dt} &= \int_{\Omega} \left[c_1\beta_h \left(S_h - \frac{c_6\mu_c}{c_1\beta_h} \right) C + c_4\beta_s \left(S_s - \frac{c_3\mu_m}{c_4\beta_s} \right) M \right] dx \\ &\leq \int_{\Omega} \left[c_1\beta_h \left(\frac{\Lambda_h}{\mu_h} - \frac{c_6\mu_c}{c_1\beta_h} \right) C + c_4\beta_s \left(\frac{\Lambda_s}{\mu_s} - \frac{c_3\mu_m}{c_4\beta_s} \right) M \right] dx \\ &\leq \int_{\Omega} \left[c_1\beta_h \frac{\Lambda_h}{\mu_h} (R_0^2 - 1) C \right] dx \end{aligned}$$

Therefore, $\frac{dL}{dt} \leq 0$ whenever $R_0 < 1$. Furthermore, $\frac{dL}{dt} = 0$ if and only if $M = C = 0$. These conditions are only satisfied by the DFE E^0 . It follows that the largest invariant set $\{(S_h, E_h, I_h, T_h, M, S_s, E_s, I_s, C) \mid \dot{L} = 0\}$ when $R_0 < 1$ is reduced to the singleton E^0 . Based on LaSalle’s Invariance Principle [30], the DFE E^0 is globally asymptotically stable when $R_0 < 1$ and unstable if $R_0 > 1$. \square

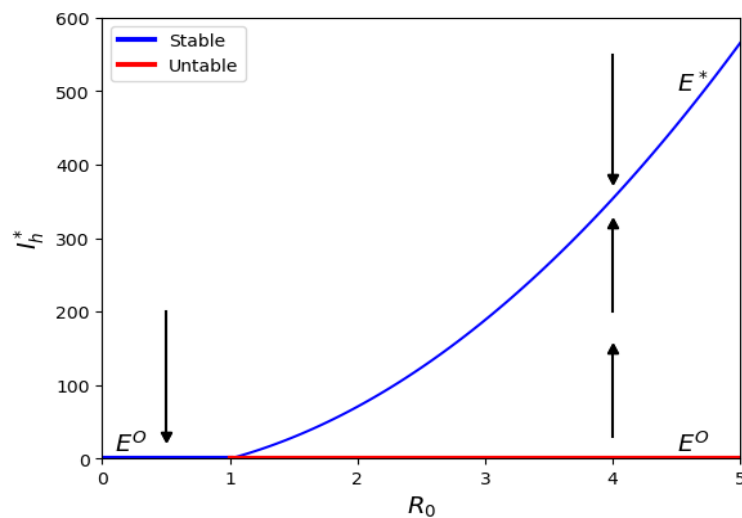


Figure 2: Bifurcation plot. This plot shows the stability of equilibrium points of the system (2.1) for $\theta(t) = 1$ as a function of R_0 . The horizontal line represents the stable and unstable states of the DFE E^0 . The half parabola represents the stable states of the EE E^* . The blue lines denote the stable states and the red lines the unstable states. The black arrows indicate the direction of the vector field.

3.4. Stability of non-autonomous dynamical system

Theorem 3.6. If $\theta(t) = (1 + \zeta e^{rt})^{-1}$, then the arbitrary equilibrium point $\bar{E} = (\bar{S}_h, \bar{E}_h, \bar{I}_h, \bar{T}_h, \bar{M}, \bar{S}_s, \bar{E}_s, \bar{I}_s, \bar{C})$ of the non-autonomous dynamical system (2.1) is uniformly stable.

Proof. We are employing the approach as in [15]. Let $X(x, t) = (S_h(x, t), E_h(x, t), I_h(x, t), T_h(x, t), M(x, t), S_s(x, t), E_s(x, t), I_s(x, t), C(x, t))$ be a solution of the system (2.1). According to the positive and boundedness of the solution in Theorem 3.1, we have

$$\limsup_{t \rightarrow +\infty, x \in \Omega} X(x, t) \leq W,$$

with $W = (w_1, w_2, w_3, w_4, w_5, w_6, w_7, w_8, w_9)$ given in (3.5). Let assume that

$$\|\phi_1\|_{C(\Omega, \mathbb{R})} \leq \frac{\Lambda_h}{\mu_h} \text{ and } \|\phi_6\|_{C(\Omega, \mathbb{R})} \leq \frac{\Lambda_s}{\mu_s}.$$

Then, for $t > 0$, we can derive the norm of the equilibrium point

$$\begin{aligned} \|E(x, t)\|_{\infty} &= \|(S_h(x, t), E_h(x, t), I_h(x, t), T_h(x, t), M(x, t), S_s(x, t), E_s(x, t), I_s(x, t), C(x, t))\|_{\infty} \\ &\leq \|W\|_{\infty} = \max\{w_1, w_6\} = \max\left\{ \frac{\Lambda_h}{\mu_h}, \frac{\Lambda_s}{\mu_s} \right\}. \end{aligned}$$

A time $t = 0$, we have:

$$\|E(x, 0)\|_{\infty} = \|(S_h(x, 0), E_h(x, 0), I_h(x, 0), T_h(x, 0), M(x, 0), S_s(x, 0), E_s(x, 0), I_s(x, 0), C(x, 0))\|_{\infty}$$

$$\begin{aligned}
 &= \left\| \left(\frac{\Lambda_h}{\mu_h}, 0, 0, 0, 0, \frac{\Lambda_s}{\mu_s}, 0, 0, 0 \right) \right\|_\infty \\
 &= \max \left\{ \frac{\Lambda_h}{\mu_h}, \frac{\Lambda_s}{\mu_s} \right\}.
 \end{aligned}$$

Let consider a class K function $\alpha(\cdot)$ such that

$$\alpha(\|E\|_\infty) = c\|E\|_\infty, \text{ with the constant } c \geq \max \left\{ 1, \frac{\Lambda_h}{\mu_h}, \frac{\Lambda_s}{\mu_s} \right\}.$$

Therefore,

$$\|E(x, 0)\|_\infty < c \Rightarrow \|E(x, t)\|_\infty < c\|E(x, 0)\|_\infty = \alpha(\|E(x, 0)\|_\infty), \quad \forall t \geq 0.$$

By applying Lemma 4.1 in [31] and the fact that all p -norms in \mathbb{R}^n are equivalent, it result that an arbitrary equilibrium point $\bar{E} = (\bar{S}_h, \bar{E}_h, \bar{I}_h, \bar{T}_h, \bar{M}, \bar{S}_s, \bar{E}_s, \bar{I}_s, \bar{C})$ of the non-autonomous dynamical system (2.1) when $\theta(t) = \theta_0(1 + \zeta e^{rt})$ is uniformly stable. □

4. Sensitivity Analysis

To assess how model parameters influence schistosomiasis spread, we employed global sensitivity analysis. This approach computed partial rank correlation coefficients (PRCC) for model parameters affecting the basic reproduction number R_0 [32], assuming statistical independence for each parameter of interest. This analysis identifies critical parameters significantly impacting the output R_0 , guiding accurate measurements.

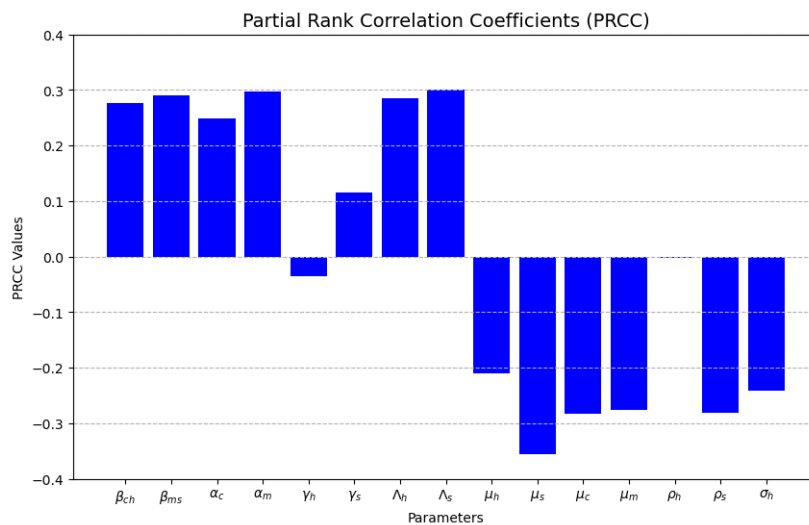


Figure 3: Plot of PRCC R_0 . The PRCC calculation was performed for R_0 using Latin Hypercube Sampling (LHS) technique. Parameters in Table 1 were sampled from uniform distributions.

Figure 3 presents the PRCC values of the model parameters. We observe that parameters such as β_{ch} , β_{ms} , γ_s , α_c , α_m , λ_h and λ_s contribute to an increase in the value of R_0 , while parameters μ_h , μ_s , μ_c , μ_m , ρ_s and σ_h are influential in reducing the burden of schistosomiasis within the population. Notably, the parameter with the highest sensitivity to R_0 is the natural death rate of the snail population μ_s . This suggests that an increase in the snail death rate effectively curtails the spread of schistosomiasis within the population.

Local sensitivity analysis is also used to examine the impact of parameter changes on disease spread using R_0 , which determines disease persistence or eradication. The normalized direct sensitivity index of R_0 with respect to a parameter v is given by :

$$S_v^{R_0} = \frac{\partial R_0}{\partial v} \times \frac{v}{R_0}. \tag{4.1}$$

This index quantifies how R_0 changes as v varies. More precisely, if v grows by $x\%$ then R_0 grows by $S_v^{R_0} \times x\%$. A positive index implies a proportional increase (decrease) in R_0 with parameter growth (reduction). Conversely, a negative index signals an opposite relationship. The local sensitivity indexes for R_0 related parameters are presented in Table 2.

Table 2: Local sensitivity index for model parameters.

Param.(v)	Λ_h	Λ_s	β_{ch}	β_{ms}	α_c	α_m	γ_h	γ_s
$S_v^{R_0}$	+0.5	+0.5	+0.5	+0.5	+0.5	+0.5	+0.000918	+0.0162
Param.(v)	μ_h	μ_s	μ_c	μ_m	ρ_s	ρ_h	σ_h	
$S_v^{R_0}$	-0.501	-0.631	-0.5	-0.5	-0.531	-0.0574	-0.442	

Table 2 demonstrates that decreasing the recruitment rates of humans and snails results in a substantial decrease in the number of human infections. Specifically, a 1% reduction in either the human or snail recruitment rate would result in a 0.5% decrease in R_0 . Conversely, a 1% increase in the treatment rate σ_h would result in a 0.442% reduction in R_0 . It is noteworthy that the parameter ρ_h , which characterizes the human death rate attributed to the infection, exerts a relatively low influence on the disease spread threshold. An augmentation of 1% in the parameter ρ_h leads to a mere 0.057% decrease in the threshold. Conversely, the natural death rate of snails, denoted as μ_s , exhibits the most significant local sensitivity index. If μ_s were to increase by 1%, R_0 would decrease notably by 0.631%. Additionally, our investigation highlights that the rates of transmission from exposure to infection, namely γ_h for humans and γ_s for snails, do not wield a significant impact on the reproductive number of the infection. This observation can be rationalized by considering the incubation period required for an exposed human or snail to become infected, which can be quite prolonged.

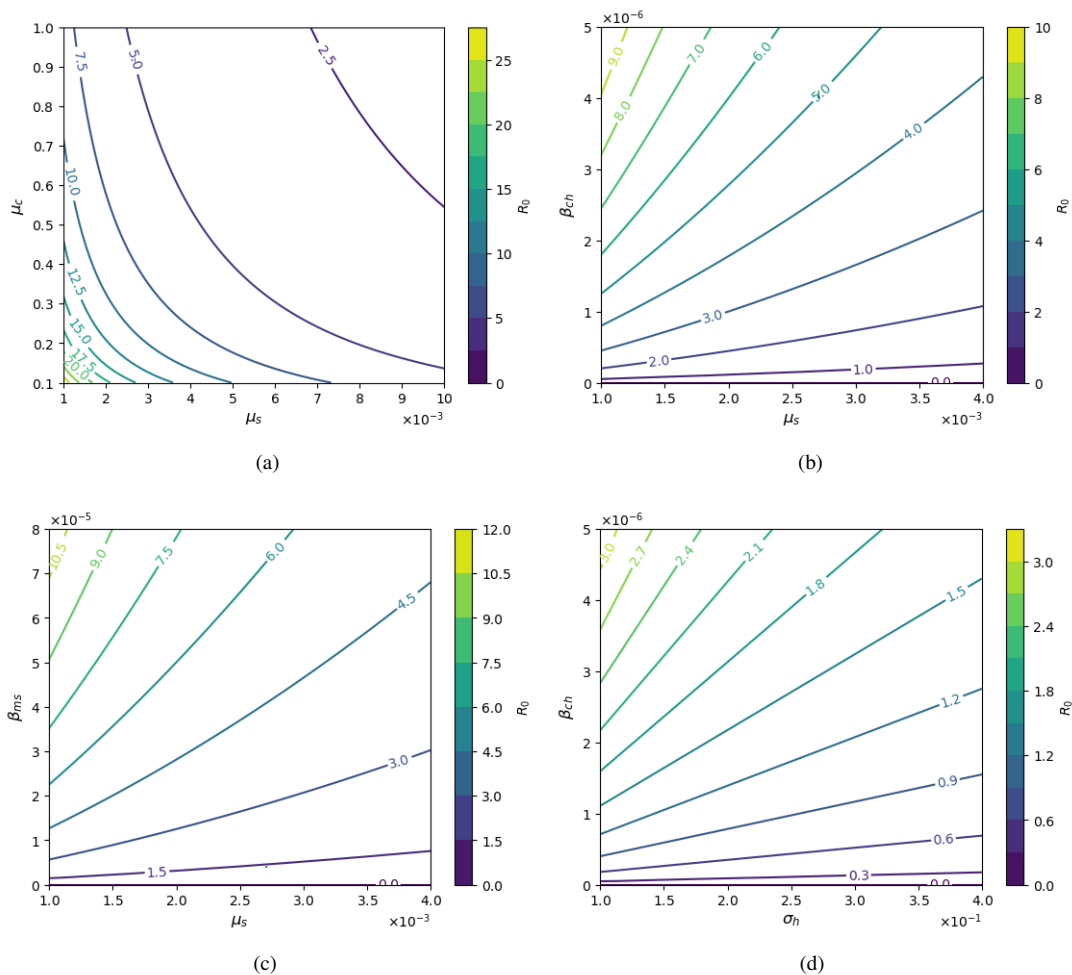


Figure 4: Contour plot of R_0 . (a) Simulated the basic reproduction number R_0 as a function of the and the natural death rate of snail μ_s and death rate of cercariae μ_c . (b) Simulated R_0 as a function of the natural death rate of snail μ_s and the infection rate of cercariae on human β_{ch} . (c) Simulated R_0 as a function of the natural death rate of snail μ_s and the infection rate of miracidia on snail β_{ms} . (d) Simulated R_0 as a function of the treatment rate of infected human σ_h and the infection rate of cercariae on human β_{ch} . The other parameters are taken at their base value in Table 1.

In Figure 4, we illustrate the influence of parameter changes μ_s , μ_c , β_{ch} , β_{ms} and σ_h on R_0 using a contour plot. When μ_s is increased while μ_c remains constant, an observable decrease in R_0 follows (see Fig 4 (a)). Conversely, a decrease in μ_s while keeping β_{ch} or β_{ms} constant results in an increase in R_0 (see Figure 4 (b)-(c)). Figure 4 (d) demonstrates that even with a high rate of infection, increasing the rate of treatment for infected humans can substantially reduce the value of R_0 . Effective control of these parameters can bring R_0 below one, meaning that disease-free equilibrium can be achieved, as proved by Theorem 3.3. This implies that disease-free equilibrium can be achieved by judiciously controlling these parameters.

5. Numerical Simulations

In this section, we conduct numerical simulations to examine disease spread in continuous space and validate theoretical analysis. Numerical computations and plots are performed in MATLAB using the built-in function `pdepe` (For more information, visit: <https://www.mathworks.com/help/matlab/ref/pdepe.html>). This function employs the finite difference method on a spatial domain $0 \leq x \leq L$ with a grid width set to 10^{-2} . This discretization transforms the system of partial differential equations (PDEs) into a large system of ordinary differential equations (ODEs), which is then solved using the built-in solver `ode15s` with a time step of $\delta t = 10^{-2}$. The 3D plots are generated using the `plotsurface` function of MATLAB, which takes as parameters the time vector, the space vector, and the numerical solution produced by the `pdepe` function.

Spatiotemporal behavior: We consider the model (2.1) with homogeneous Neumann boundary conditions (2.4). For convenience, we set $\Omega = [0, 1]$. In our model, human population movement is influenced by factors like migration and commuting behaviors, and it is assumed to occur downstream along the river, reflecting the natural flow of infected individuals and the spread of contamination. Snails, acting as intermediate hosts, can move within the water, primarily influenced by water currents and environmental factors. This movement contributes to the downstream distribution of cercariae. Miracidia, the parasite larvae, and cercariae, the infectious stage, are carried downstream by water flow, facilitating their transmission to susceptible snails and humans in downstream areas. To capture such movement dynamics, we fix the following diffusion coefficients in units of $\text{m}^2 \text{day}^{-1}$: $d_1 = 0.1$, $d_2 = 0.05$, $d_3 = 0.02$, $d_4 = 0.1$, $d_5 = 0.0005$, $d_6 = 0.001$, $d_7 = 0.0005$, $d_8 = 0.0003$, $d_9 = 0.0002$.

Additionally, we adopt the subsequent initial conditions: $S_h(0) = 0.99 \frac{\Lambda_h}{\mu_h} - 200 \cos(2\pi x)$, $E_h(0) = 0$, $I_h(0) = 0.01 \frac{\Lambda}{\mu_s} - 50 \cos(2\pi x)$, $T_h(0) = 0$, $M = 10$, $S_s(0) = 0.99 \frac{\Lambda_s}{\mu_s} - 3 \cos(2\pi x)$, $E_s(0) = 0$, $I_s(0) = 0.01 \frac{\Lambda_s}{\mu_s} - 2 \cos(2\pi x)$, $C = 10$.

We divide the simulations into different cases corresponding to the stability of each one of the equilibrium points of the model (2.1) as follows:

- Case 1:** We consider the values $\beta_{ch} = 2 \times 10^{-6}$, $\beta_{ms} = 3 \times 10^{-5}$, $\alpha_c = 1.5$, $\alpha_m = 2.96$, $\mu_s = 6 \times 10^{-3}$, $\mu_c = 1.01$, $\mu_m = 5$ and $\theta(t) = 1$, the other parameters are given in a Table 1. The corresponding threshold is $R_0 = 0.5839 < 1$ and from Theorem 3.5 the DFE is GAS. As depicted in Figure 5, the numbers of infected individuals $I_h(t, x)$ and infected snails $I_s(t, x)$ converge to zero.
- Case 2:** We consider all the value the parameter values given in a Table 1 with $\theta(t) = 1$. The corresponding threshold is $R_0 = 4.989 > 1$ and it follows from Theorem 3.4 that the EE is LAS. As shown in Figure 6, the numbers of infected individuals $I_h(t, x)$ and infected snails $I_s(t, x)$ converge to the endemic points I_h^* and I_s^* , respectively.
- Case 3:** We consider the same parameters as presented in Table 1, but with $\theta(t) = (1 + \zeta e^{rt})^{-1}$, where $\zeta = 0.02$ and $r = 0.005$. As demonstrated in Theorem 3.6, the equilibrium of the non-autonomous dynamical system displays uniform stability. Illustrated in Figure 7, the intervention function's effect, $\theta(t)$, leads to a gradual reduction of the reproduction number below 1 over time. Consequently, both the numbers of infected individuals, $I_h(t, x)$ and infected snails, $I_s(t, x)$, decrease and converge to zero over time, while the populations of susceptible humans and snails increase. We find that the spatio-temporal evolution of exposed and infected humans are similar, indicating that human interventions have the same effect on exposed individuals as they do on infected individuals.

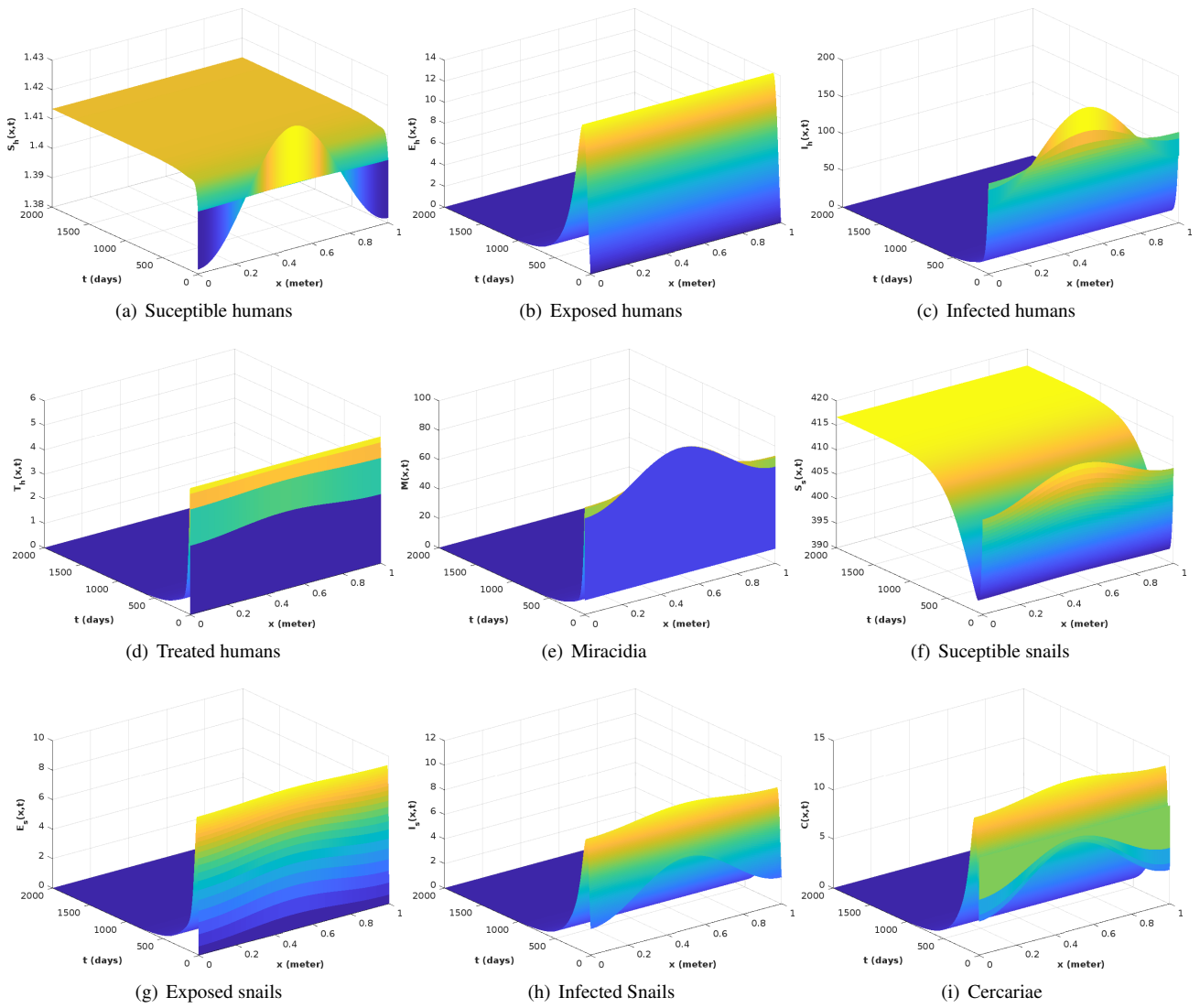


Figure 5: Spatiotemporal evolution of schistosomiasis transmission when $R_0 < 1$ and $\theta(t) = 1$. The disease-free equilibrium E^0 is globally asymptotically stable.

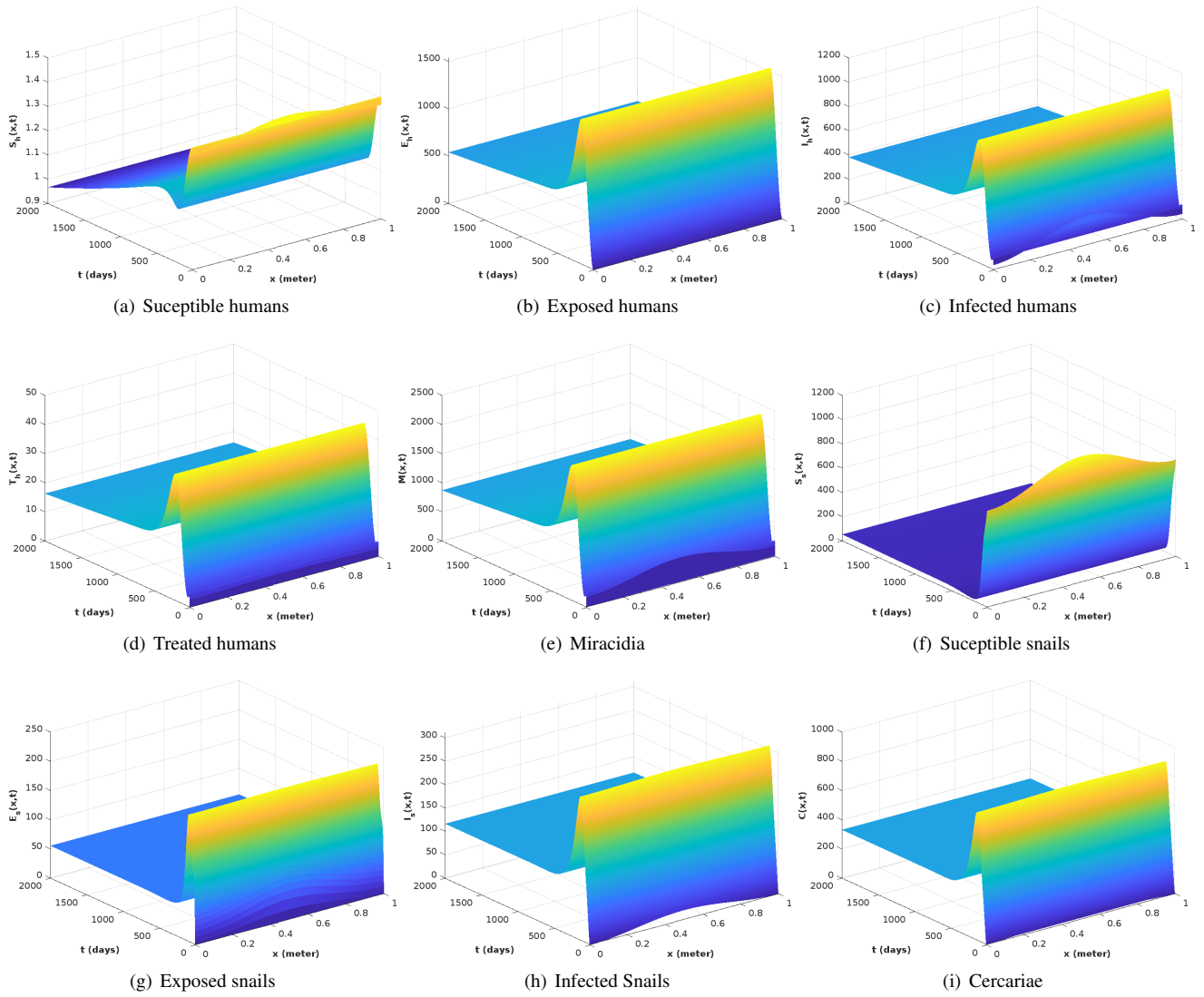


Figure 6: Spatiotemporal evolution of schistosomiasis transmission when $R_0 > 1$ and $\theta(t) = 1$. The endemic equilibrium E^* is globally asymptotically stable.

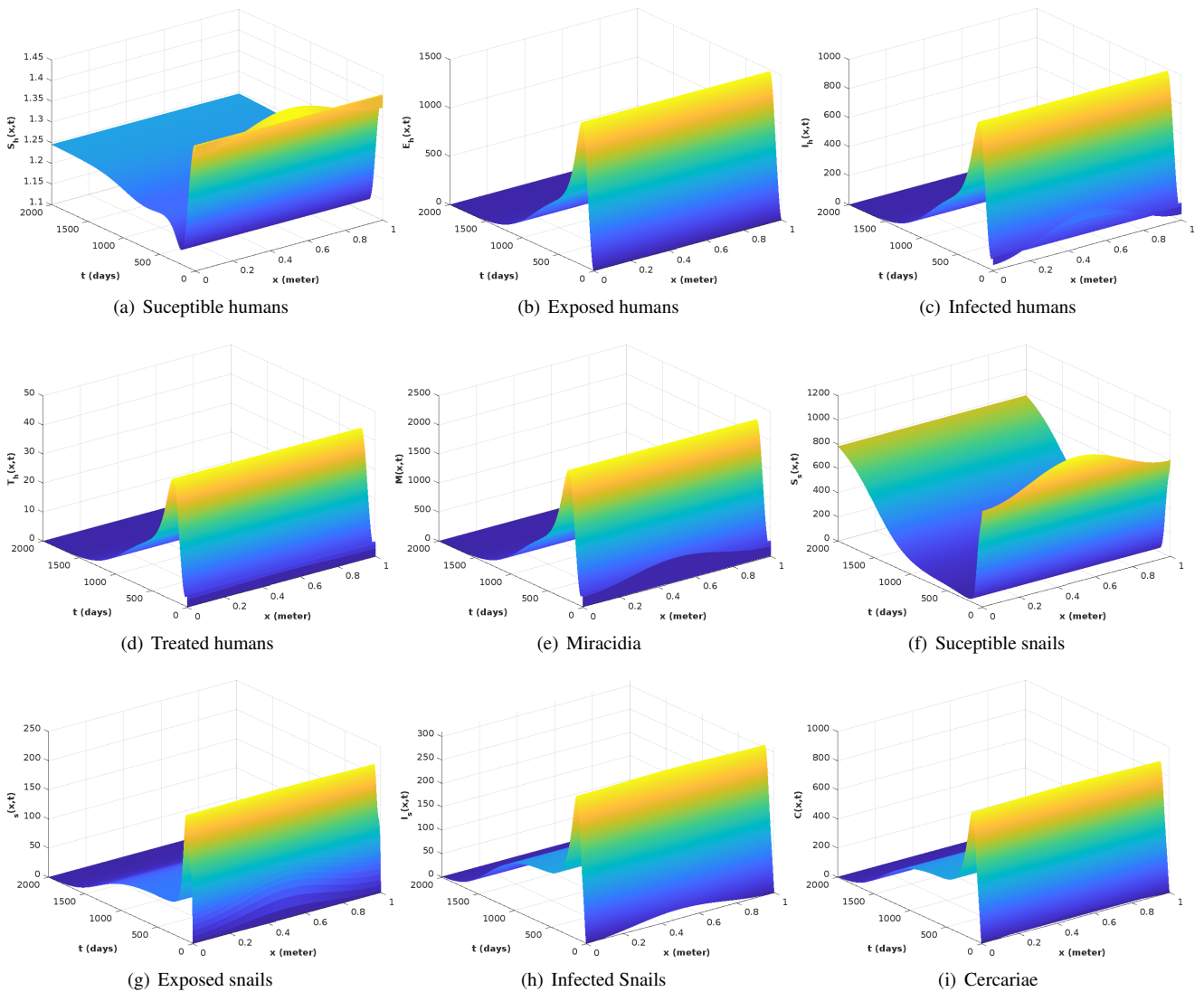


Figure 7: Spatiotemporal evolution of schistosomiasis transmission when $R_0 > 1$ and human intervention $\theta(t) = (1 + \zeta e^{rt})^{-1}$. The arbitrary equilibrium of the non-autonomous system is uniformly stable

The simulations above illustrate that in a homogeneous system, while the early phase may exhibit variation depending on the spatial location x , the eventual state of the infectious disease appears to be independent of its dispersal rate.

Control Strategies: Here, an examination of the temporal evolution of the disease progression under different control measures, namely Mass Drug Administration (MDA) and human interventions is conducted. Figure 8 illustrates the progression of disease prevalence while varying treatments for infected humans. For all cases, the baseline parameter values listed in Table 1 are used and only manipulate the parameters σ_h (infected treatment rate) and β_{ch} (reinfection rate). The graphs in Figure 8 are generated using the ODE version of the equation (2.1), with each curve representing the proportion (in percentage) of infected individuals over the total population.

Figure 8 demonstrates the impact of human interventions on the spread of *Schistosoma*. The curves colored in red, yellow, green and blue represent infection prevalence with no treatment ($\sigma_h \approx 0$), low treatment ($\sigma_h = 0.03$), moderate treatment ($\sigma_h = 0.12$) and high treatment ($\sigma_h = 0.25$), respectively. Notably, the most severe outbreaks manifest during the early phase across the four scenarios mentioned. These findings suggest that MDA is an effective control strategy not only in the initial stages of transmission but also throughout the transmission process (see Fig 8 (a)-(c)). Applying appropriate treatment to infected individuals can substantially diminish disease prevalence. Nevertheless, as depicted in Fig 8 (a)-(c), relying solely on MDA becomes insufficient when the reinfection rate becomes high. Therefore, it becomes imperative to encourage individuals to adopt additional control measures such as avoiding contact with contaminated water through wading, swimming and other activities, along with implementing improved sanitation and securing access to clean water. Fig 8 (d) underscores that combining MDA with human interventions ($\zeta = 0.02$ and $r = 0.005$) can lead to a significant reduction in prevalence.

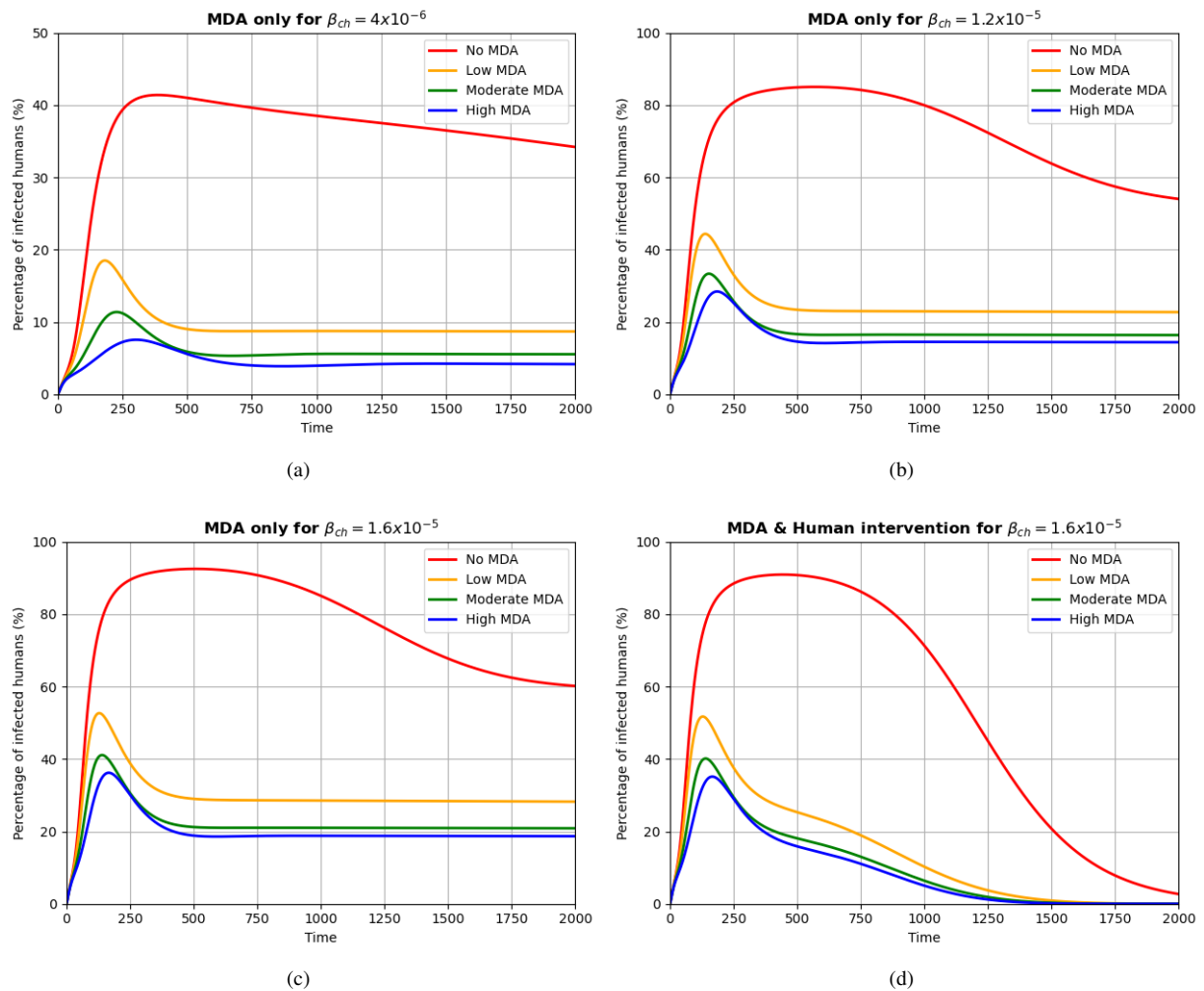


Figure 8: Influence of varying MDA rate on infection prevalence.

6. Conclusion

In this paper, an enhanced mathematical model has been developed utilizing diffusion equations to depict the dynamics of schistosomiasis, thereby expanding upon a previously established framework. By integrating both the influence of treated individuals and the temporal function of human interventions, the extended model has been thoroughly analyzed both temporally and spatially, delving into critical aspects such as the existence, uniqueness, and positivity of solutions, as well as the existence and stability of endemic and disease-free equilibria, contingent upon the threshold value of the basic reproduction number, R_0 . It has been demonstrated that when $R_0 < 1$, the global asymptotic stability of the disease-free equilibrium has been conclusively established. Conversely, for $R_0 > 1$, the endemic equilibrium has been firmly established as locally stable within the autonomous system. Furthermore, the results have been extended to non-autonomous systems, showcasing the uniform stability of any arbitrary equilibrium, irrespective of the value of R_0 . Additionally, a comprehensive sensitivity analysis of R_0 has been conducted, employing PRCC and the local sensitivity index to unravel the intricate dynamics influenced by individual parameters. It has been determined that a 1% increase in the treatment rate σ_h would result in a 0.442% reduction in R_0 . The theoretical findings have been rigorously validated through numerical simulations, which corroborate the conclusions drawn from the qualitative analysis, notably emphasizing the profound impact of various control measures. These findings underscore the efficacy of Mass Drug Administration (MDA) as a control strategy not only during the initial stages of transmission but also throughout the transmission process. However, it has been elucidated through numerical simulations that relying solely on MDA becomes inadequate when the reinfection rate escalates. Consequently, it becomes imperative to advocate for the adoption of additional control measures by individuals, such as avoiding contact with contaminated water through activities like wading and swimming, in addition to implementing improved sanitation and securing access to clean water. Furthermore, the combined implementation of mass drug administration (MDA) and targeted human interventions has been identified as a potent approach, substantially diminishing the prevalence of infection and aligning with the targets set by the World Health Organization. This holistic strategy not only addresses the immediate challenges posed by schistosomiasis but also lays the groundwork for sustainable long-term management of the disease. In our future research, we plan to explore the optimization of intervention strategies by considering socioeconomic factors, geographical variations, and the evolution of drug resistance.

Furthermore, incorporating predictive modeling techniques could facilitate the development of proactive intervention strategies, thereby enhancing the overall effectiveness of schistosomiasis control efforts.

Declarations

Acknowledgements: The author would like to express his deep thanks to the anonymous reviewers for their helpful comments and suggestions, and to the editor for his very kindly and patient technical assistance during the preparation of the final version of the article.

Conflict of Interest Disclosure: The authors declare no conflict of interest.

Copyright Statement: Authors own the copyright of their work published in the journal and their work is published under the CC BY-NC 4.0 license.

Supporting/Supporting Organizations: This research received no external funding.

Ethical Approval and Participant Consent: This article does not contain any studies with human or animal subjects. It is declared that during the preparation process of this study, scientific and ethical principles were followed and all the studies benefited from are stated in the bibliography.

Plagiarism Statement: This article was scanned by the plagiarism program. No plagiarism detected.

Availability of Data and Materials: Data sharing not applicable.

Use of AI tools: The author declares that he has not used Artificial Intelligence (AI) tools in the creation of this article.

ORCID

Dhorasso Temfack  <https://orcid.org/0009-0007-0630-7504>

References

- [1] World Health Organization, *WHO Guideline on Control and Elimination of Human Schistosomiasis*, (2022). [Web]
- [2] World Health Organization, *Ending the Neglect to Attain the Sustainable Development Goals*, (2020). [Web]
- [3] E.J. Allen and H.D. Victory, *Modelling and simulation of a schistosomiasis infection with biological control*, Acta Trop., **87**(2) (2003), 251–267. [CrossRef] [Scopus] [Web of Science]
- [4] A.G. Ross, D. Vickers, G.R. Olds, S.M. Shah and D.P. McManus, *Katayama syndrome*, Lancet Infect. Dis., **7**(3) (2007), 218–224. [CrossRef] [Scopus] [Web of Science]
- [5] E.Y.-Y. Li, D. Gurarie, N.C. Lo, X. Zhu and C.H. King, *Improving public health control of schistosomiasis with a modified WHO strategy: A model-based comparison study*, Lancet Glob. Health, **7**(10) (2019), e1414–e1422 [CrossRef] [Scopus] [Web of Science]
- [6] G. Macdonald, *The dynamics of helminth infections, with special reference to schistosomes*, Transactions of the Royal Society of Tropical Medicine and Hygiene, Trans. R. Soc. Trop. Med. Hyg., **59**(5) (1965), 489–506 [CrossRef] [Scopus]
- [7] C.E. Madubueze, Z. Chazuka, I.O. Onwubuya, F. Fatmawati and C.W. Chukwu, *On the mathematical modeling of schistosomiasis transmission dynamics with heterogeneous intermediate host*, Front. Appl. Math. Stat., **8**, 1020161. [CrossRef] [Scopus] [Web of Science]
- [8] S. Wang and R.C. Spear, *Exploring the contribution of host susceptibility to epidemiological patterns of schistosoma japonicum infection using an individual-based model*, Am. J. Trop. Med. Hyg., **92**(6) (2015), 1245–1252. [CrossRef] [Scopus] [Web of Science]
- [9] M. Graham, D. Ayabina, T.C. Lucas, B.S. Collyer, G.F. Medley, T.D. Hollingsworth and J. Toor, *Schistox: An individual-based model for the epidemiology and control of schistosomiasis*, Infect. Dis. Model., **6** (2021), 438–447. [CrossRef] [Scopus] [Web of Science]
- [10] M. Ciddio, L. Mari, S.H. Sokolow, G.A. De Leo, R. Casagrandi and M. Gatto, *The spatial spread of schistosomiasis: A multidimensional network model applied to Saint-Louis region, Senegal*, Adv. Water Resour., **108** (2017), 406–415. [CrossRef] [Scopus] [Web of Science]
- [11] T. Manyangadze, M.J. Chimbari, M. Gebreslasie, P. Ceccato and S. Mukaratirwa, *Modelling the spatial and seasonal distribution of suitable habitats of schistosomiasis intermediate host snails using MaxEnt in Ndumo area, KwaZulu-Natal Province, South Africa*, Parasit. Vectors, **9**(1) (2016), 1–10, 572 [CrossRef] [Scopus] [Web of Science]
- [12] H. Zhang, P. Harvim and P. Georgescu, *Preventing the spread of schistosomiasis in Ghana: possible outcomes of integrated optimal control strategies*, J. Biol. Syst., **25**(4) (2017), 625–655 [CrossRef] [Scopus] [Web of Science]
- [13] E. Kanyi, A.S. Afolabi and N.O. Onyango, *Mathematical modeling and analysis of transmission dynamics and control of schistosomiasis*, J. Appl. Math., **2021** (2021), 6653796. [CrossRef] [Scopus]
- [14] J. M. Haugh, *Analysis of reaction-diffusion systems with anomalous subdiffusion*, Biophys. J., **97**(2) (2009), 435–442. [CrossRef] [Scopus] [Web of Science]
- [15] R. Li, Y. Song, H. Wang, G.-P. Jiang and M. Xiao, *Reactive–diffusion epidemic model on human mobility networks: Analysis and applications to COVID-19 in China*, Phys. A: Stat. Mech. Appl., **609** (2023), 128337. [CrossRef] [Scopus] [Web of Science]
- [16] W. Nur, Trisilowati1, A. Suryanto and W.M. Kusumawinahyu, *Mathematical model of schistosomiasis with health education and molluscicide intervention*, J. Phys. Conf. Ser., **1821**(1) (2021), 012033 [CrossRef] [Scopus]
- [17] M. Diaby, *Stability analysis of a schistosomiasis transmission model with control strategies*, Biomath, **4**(1) (2015), 1-13. [CrossRef]
- [18] E.T. Chiyaka and W. Garira, *Mathematical analysis of the transmission dynamics of schistosomiasis in the human-snail hosts*, J. Biol. Syst., **17**(3) (2009), 397–423. [CrossRef] [Scopus] [Web of Science]
- [19] J. Zwang and P.L. Olliaro, *Clinical efficacy and tolerability of praziquantel for intestinal and urinary schistosomiasis—a meta-analysis of comparative and non-comparative clinical trials*, PLoS Negl. Trop. Dis., **8**(11) (2014), e3286. [CrossRef] [Scopus] [Web of Science]
- [20] R. Redlinger, *Existence theorem for semilinear parabolic systems with functionals*, Nonlinear Anal., **8**(6) (1984), 667–682. [Scopus]
- [21] W. Wang and X.-Q. Zhao, *Basic reproduction numbers for reaction diffusion epidemic models*, SIAM J. Appl. Dyn. Syst., **11**(4) (2012), 1652–1673. [CrossRef] [Scopus] [Web of Science]
- [22] Y. Song and T. Zhang, *Global stability of the positive equilibrium of a mathematical model for unstirred membrane reactors*, B. Korean Math. Soc., **54**(2) (2017), 383–389. [CrossRef] [Scopus] [Web of Science]
- [23] B. Kammegne, K. Oshinubi, O. Babasola, O. Peter, O. Longe, R. Ogunrinde, E. Titiloye, R. Abah and J. Demongeot, *Mathematical modelling of the spatial distribution of a COVID-19 outbreak with vaccination using diffusion equation*, Pathogens, **12**(1) (2023), 88. [CrossRef] [Scopus] [Web of Science]

- [24] R. Peng and M. Wang, *Global stability of the equilibrium of a diffusive Holling-Tanner prey-predator model*, Appl. Math. Lett., **20**(6) (2007), 664–670. [[CrossRef](#)] [[Scopus](#)] [[Web of Science](#)]
- [25] J. Kim, W. Su and Y. Song, *On stability of a polynomial*, J. Appl. Math. Inform., **36**(3-4) (2018), 231-236. [[CrossRef](#)] [[Web of Science](#)]
- [26] J.M. Heffernan, R.J. Smith and L.M. Wahl, *Perspectives on the basic reproductive ratio*, J. R. Soc. Interface., **2**(4) (2005), 281–293. [[Cross-Ref](#)] [[Scopus](#)] [[Web of Science](#)]
- [27] H.W. Hethcote and H.R. Thieme, *Stability of the endemic equilibrium in epidemic models with subpopulations*, Math. Biosci., **75**(2) (1985), 205–227. [[CrossRef](#)] [[Scopus](#)] [[Web of Science](#)]
- [28] C. Tadmon and S. Foko, *A transmission dynamics model of COVID-19: Case of Cameroon*, Infect. Dis. Model., **7**(2) (2022), 211–249. [[CrossRef](#)] [[Scopus](#)] [[Web of Science](#)]
- [29] C.N.T. Mfangnia, H.E.Z. Tonnang, B. Tsanou and J. Herren, *Mathematical modelling of the interactive dynamics of wild and microsporidia MB-infected mosquitoes*, Math. Biosci. Eng., **20**(8) (2023), 15167–15200. [[CrossRef](#)] [[Scopus](#)] [[Web of Science](#)]
- [30] J. La Salle, *The Stability of Dynamical Systems*, Philadelphia, PA, USA: SIAM, (1976). [[Web](#)]
- [31] H. Marquez, *Nonlinear Control Systems: Analysis and Design*, Hoboken, New Jersey: John Wiley & Sons, Inc., (2003). [[Web](#)]
- [32] S. Marino, I.B. Hogue, C.J. Ray and D.E. Kirschner, *A methodology for performing global uncertainty and sensitivity analysis in systems biology*, J. Theor. Biol., **254**(1) (2008), 178–196. [[CrossRef](#)] [[Scopus](#)] [[Web of Science](#)]

Fundamental Journal of Mathematics and Applications (FUJMA), (Fundam. J. Math. Appl.)

<https://dergipark.org.tr/en/pub/fujma>



All open access articles published are distributed under the terms of the CC BY-NC 4.0 license (Creative Commons Attribution-Non-Commercial 4.0 International Public License as currently displayed at <http://creativecommons.org/licenses/by-nc/4.0/legalcode>) which permits unrestricted use, distribution, and reproduction in any medium, for non-commercial purposes, provided the original work is properly cited.

How to cite this article: D. Temfack, *Mathematical modeling of Schistosomiasis transmission using reaction-diffusion equations*, Fundam. J. Math. Appl., **7**(2) (2024), 118-137. DOI 10.33401/fujma.1412958